Nr 10 (537–616) PAŹDZIERNIK 2024 Tom LXIX

POLIMERY

# Effect of carbon nanotubes on the structure and selected properties of polymer-bitumen binders

**Andrii Bieliatynskyi**[1] (ORCID ID: 0000-0002-2158-512X), **Olena Bakulich**[2] (0000-0002-5700-0576), **Viacheslav Trachevskyi**[3), *)] (0000-0002-3916-9116), **Mingyang Ta**[4] (0000-0003-4283-6554)

DOI: https://doi.org/10.14314/polimery.2024.10.1

**Abstract**: The effect of CNTs on the structure, rheological and mechanical properties of polymer-bitumen binders (PBB) was investigated. CNTs were obtained by pyrolysis of acetylene, toluene, dichloromethane, acetonitrile and a mixture of carbon disulfide and dichloromethane. Transmission electron microscopy (TEM), X-ray diffraction (XRD), Raman spectroscopy and thermal analysis (DSC, TGA) were used to characterize CNTs. It was proven that CNTs stabilize PBBs, slowing down the degradation processes. Compared to the reference sample, the use of CNTs resulted in a slight decrease in both the tensile strength of the asphalt after 3 h of heating at 20°C (4%) and the compressive strength at 50°C (3%).

**Keywords**: composite, chemical composition, nanomaterials, modifiers, asphaltenes.

## Wpływ nanorurek węglowych na strukturę i wybrane właściwości lepiszczy polimerowo-bitumicznych

**Streszczenie:** Zbadano wpływ CNT na strukturę, właściwości reologiczne i mechaniczne lepiszczy polimerowo-bitumicznych (PBB). CNT otrzymano w wyniku pirolizy acetylenu, toluenu, dichlorometanu, acetonitrylu oraz mieszaniny disiarczku węgla i dichlorometanu. Do charakterystyki CNT zastosowano transmisyjną mikroskopię elektronową (TEM), dyfrakcję rentgenowską (XRD), spektroskopię Ramana oraz analizę termiczną (DSC, TGA). Wykazano, że CNT stabilizują PBB, spowalniając procesy degradacji. W porównaniu z próbką odniesienia zastosowanie CNT skutkowało niewielkim zmniejszeniem zarówno wytrzymałości na rozciąganie asfaltu po 3 h ogrzewania w temperaturze 20°C (4%), jak i wytrzymałości na ściskanie w temperaturze 50°C (3%).

**Słowa kluczowe:** kompozyt, skład chemiczny, nanomateriały, modyfikatory, asfalteny.

Materials conventionally employed for structural purposes exhibit limitations in their properties, prompting ongoing advancements in materials science to engineer composite structures. The chemical composition of individual components is pivotal, but equally crucial is their atomic structure and interrelation, constituting the inter-

---

1) School of Civil Engineering, North Minzu University, 750021, 204 Wenchang Road, Yinchuan, NingXia, P.R. China.

2) Faculty of Management, Logistic and Tourism, National Transport University, 01010, 1 Mykhailo Omelianovych-Pavlenko Str., Kyiv, Ukraine.

3) Institute of Macromolecular Chemistry, National Academy of Sciences of Ukraine 02155, 48 Kharkivske Hwy, Kyiv, Ukraine.

4) School of Civil Engineering, North Minzu University, 750021, 204 Wenchang Road, Yinchuan, NingXia, P.R. China.

*) Author for correspondence: meches49@ukr.net

nal architecture of the composite. This internal arrangement affords control over the electronic properties of the resultant material. The diverse geometries possible in hybrid structures, comprising elements such as polyparaphenylene fibers, carbon nanotubes, graphene, graphene oxide, nanocrystalline cellulose fibers, nanoclusters, and graphene, exemplify materials composed of disparate components. These components, though often dissimilar, synergistically contribute to the composite's unique properties [1]. Composites result from the interaction of chemically distinct constituents, forming a spatial structure that deviates from the original reagents' structures but frequently emulates certain properties and functions of the initial structures [2, 3].

In natural composites, inorganic particle sizes typically range from microns to millimeters, resulting in visible heterogeneity. Reducing inorganic particle sizes to nanometer scales enhances composite homogeneity, yielding improved or novel properties, termed hybrid nanostructures. Inorganic components include nanoparticles, macromolecules, nanotubes, and layered substances, offering numerous combinations with organic counterparts. Carbon nanoparticles are promising for enhancing physical, mechanical, and functional attributes [4]. Functionalized carbon nanoparticles function as modifiers in polymer composite materials, regulating curing and plasticization processes [5, 6]. They alter the composite's chemical composition, impart functional properties, and enable 3D reinforced hybrid nanocomposite production.

Thanks to the ability to control the mechanical, chemical, and electrical properties in the composite, graphene oxide and carbon nanotubes are of great interest among scientists. Graphene structure consists of a monolayer of $sp^2$–hybridized carbon atoms with a two-dimensional (2D) honeycomb lattice. This structure allows for the construction of other types of materials, such as fullerene, carbon nanotubes (CNTs), etc. With the discovery of new members of the graphene family, such as graphene oxide (GO), reduced graphene oxide (rGO) (Fig. 1), graphene quantum dots (GQD), the investigation of the graphene derivatives in the field of chemistry, physics and biomedicine were possible.

Graphene and its derivatives can be easily modified with small molecular dyes, polymers, nanoparticles (NPs), drugs or biomolecules to produce nanomaterials for different bioimplantation regimes. Graphene-based fibers demonstrate excellent flexibility and electrical conductivity, due to the linear fibrous structure. In addition, given the large amount of natural graphite and the established spinning technique, graphene-based fibers derived from graphene oxide (GO) are becoming one of the most promising candidates for working as flexible electrodes [7]. However, graphene fibers are known for their natural hydrophobicity, which can lead to a low specific surface area and poor compatibility with the electrolyte, resulting in poor electrochemical properties.

Carbon nanotubes are regarded as one of the mechanically strongest materials. This phenomenon is associated with the covalent force between individual $sp^2$ carbon atoms [8]. Although the strength of individual shells of carbon nanotubes is extremely high, weak resistance to displacement between adjacent shells and pipes leads to a significant decrease in the effective force. The conductive properties of carbon nanotubes have a strong functional dependence on chemical doping, mechanical deformation, and atomic structure. It is also noted

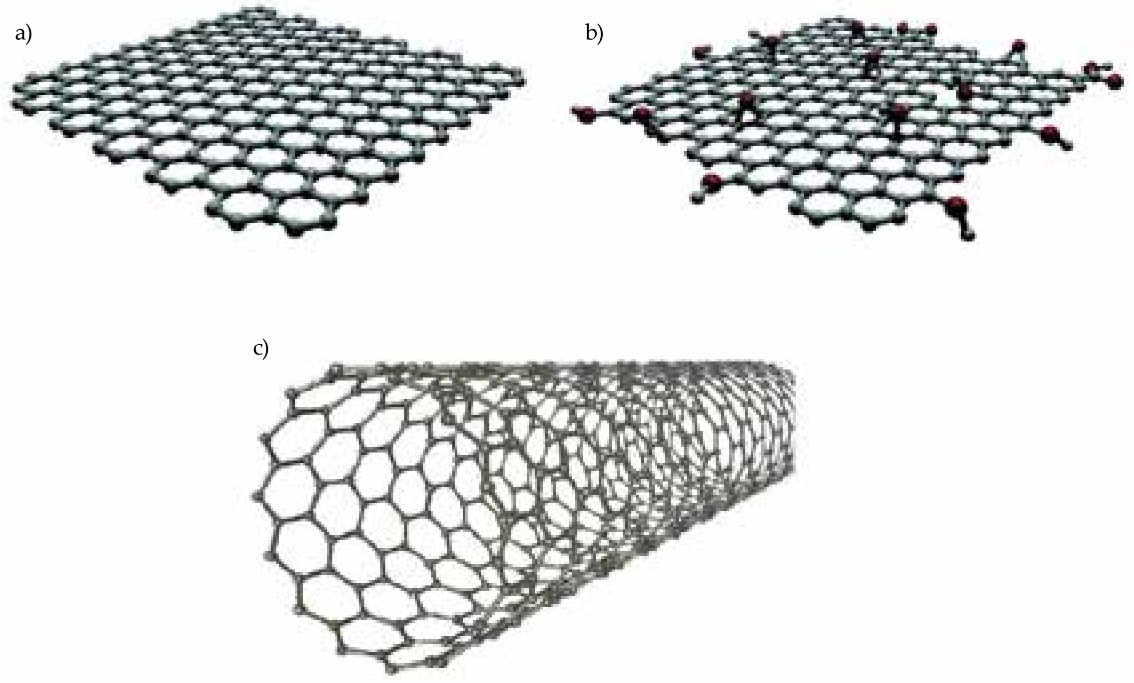

**Fig. 1. Structures of carbon nanostructures: a) graphene, b) graphene oxide, c) carbon nanotubes**

that carbon nanotubes have useful photoluminescence properties. Recently, several types of technologies have been developed to produce carbon nanotubes in significant quantities, such as arc discharge, laser ablation and chemical vapor deposition. Most of these processes occur in a vacuum or with inert gases. Controlled synthesis of carbon nanotubes opens exciting opportunities for their use in nanotechnology, surface chemistry and photochemistry, molecular sensors.

Functionalization of carbon nanotubes using the covalent method allows for the placement of useful functional groups on the surface of carbon nanotubes. Unfortunately, this method has two main drawbacks. Firstly, several faults in the side carbon walls of the nanotubes invariably emerge during the functionalization procedure. It is noted that in severe situations, the nanotubes break into smaller pieces [9-11]. These damaging effects can lead to a strong degradation of the mechanical properties of carbon nanotubes, as well as the destruction of the $\pi$–electron structure in carbon nanotubes. It can result in degradation of the CNTs conductive properties since defective areas scatter phonons and electrons responsible for the thermal and electrical conductivities of carbon nanotubes. Secondly, strong oxidizers or concentrated acids that are usually environmentally hazardous, are commonly used to functionalize CNTs [12, 13]. Recent experiments have demonstrated that multi-walled carbon nanotubes can be used to dope the functional conjugation of a polyaniline and a conjugated luminescent polymer. The electron structure of the functional conjugated polymer, as well as other types of leading polymers, are modified by the presence of CNTs, indicating a strong bond of carbon nanotube polymers.

In another system, wall-mounted carbon nanotubes affected the electrical properties of the polymer. The interphase characteristics of carbon nanotube polymers directly affect the efficiency of CNT amplification while improving the mechanical, thermal, and electrical properties of the carbon nanotube polymer nanocomposite. Optimal interaction of carbon nanotube polymers is a critical factor for achieving the full potential of CNTs in nanocomposites. Although a wide range of characteristic parameters have been reported, there are conflicting reports showing that the effect of carbon nanotubes on a particular property is not observed, improving them, or even exacerbating them. These conflicting conclusions derived from differences between material characteristics and nanocomposite processing conditions. In addition, there are a number of other parameters, such as the curvature of carbon nanotubes, which plays a significant role in achieving optimal nanocomposite configuration [14]. The interaction of carbon nanotube polymers depends on the characteristics of both constituents and how they interact with each other. Carbon nanotube-polymer composites do not have high enough electrical conductivity to replace metal wiring. However, there are a number of applications where the electrical conductivity requirement is not as stringent.

The properties of graphene, graphene oxide and carbon nanotube are not only well studied, but they are already widely used in industry and science as components of hybrid nanostructures in the composition of sensors, electrodes, etc. The future of technology depends on the effectiveness of the research system, which will ensure that all parts of the process of creating artificial materials with specified properties are properly implemented. One of these links is theoretical calculations, including the first predictive principles of electronic and chemical properties of an artificial structure to create its experimental sample. This stage is necessary given the complexity and high cost of manufacturing composite structures under development. According to this, the meta-development of a new chemical composition of composite materials filled with carbon nanotubes with high physical, mechanical, and operational characteristics was delivered.

The performance properties of any building material are determined by its composition and structure. Meanwhile, the composition depends on the type and quantitative ratio of the components of the mixture, and the structure is determined by the nature of the bonds between the astringent and contacting particles, their shape and relative position relative to each other. Therefore, numerous studies in this area are aimed at identifying the relationship between properties and structural features corresponding to them, as well as analyzing the processes at the micro level, which allows regulating the physicochemical properties of the materials under study [6, 15, 16]. Rybiev developed two concepts of the structure formation of artificial building conglomerates based on the experience of studies of changes in the properties of building materials. These concepts include the idea that there is a direct relationship between the strength indicators of the composite and its binder, while achieving optimal formulations. Thus, the pattern established for one material is transferred to other materials, if their structures are optimal [8, 17].

Usually, organo-mineral composites of all kinds are highly concentrated disperse systems, which allows them to be considered as objects of physical and chemical mechanics of disperse systems. Effective structure formation management is based on an optimal combination of two factors: an advanced interfacial surface of a finely dispersed mineral part and a large concentration of the dispersed phase in a liquid (dispersion) medium. Carbon nanotubes, which will be the liquid phase of the binder, can be utilized as an example of nanomodification of bitumen. This will result in the transfer of modified properties to the main composite, changing its properties and chemical bonding directly [18, 19]. The main composite using bitumen as a binder is asphalt concrete. The modification of the binder is made by carbon nanotubes, as the most progressive type of modifier.

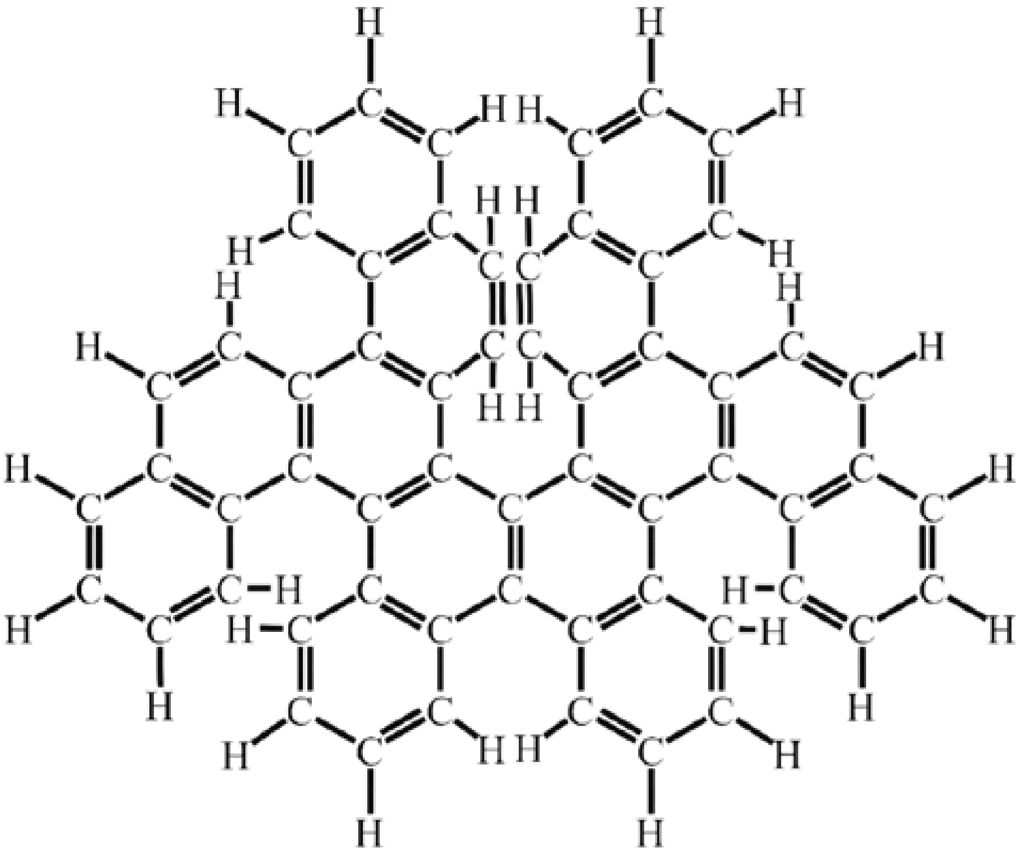

**Fig. 2. Bitumen structure**

The chemical composition of the bitumen group is the separation of bitumen by adsorption into conditional fractions, which are complex compounds combined based on solubility [20, 21]. The structure of bitumen is presented in Fig. 2.

The average elemental composition of asphaltenes is (in wt %): C – 82±3, H – 8.1±0.7, O – 5, N – 2-19, Ni – 0.01–0.02 with microquantities of Fe, Ca, Mg and Cu. More detailed studies of asphaltenes and oil residues using modern methods, such small-angle neutron scattering (SANS), X-ray scattering, ultrasonic spectroscopy, nuclear magnetic resonance (NMR), dynamic light scattering (DLS), fluorescence correlation spectroscopy (FCS), fluorescence depolarization, reverse ebullioscopy, gel permeation chromatography (GPC), etc. Such measurements made it possible to establish their main morphostructural features, as well as the initial dimensions of the asphaltene molecule, which start from 1 nm [22, 23].

Due to the polarity of the asphaltene molecules, they are structured into associates in the form of bundles, which are arranged parallel to each other. The structure of asphaltenes resembles the structure of graphite (Fig. 3).

Bitumen can be described as a dispersion system composed of various high-molecular-weight petroleum compounds and their derivatives, including oils, resins, and asphaltenes. The asphaltenes form pseudospherical particles, acting as solid-phase nuclei with colloidal dimensions. This interpretation aligns with studies suggesting that asphaltene "embryos" represent the smallest, inde-

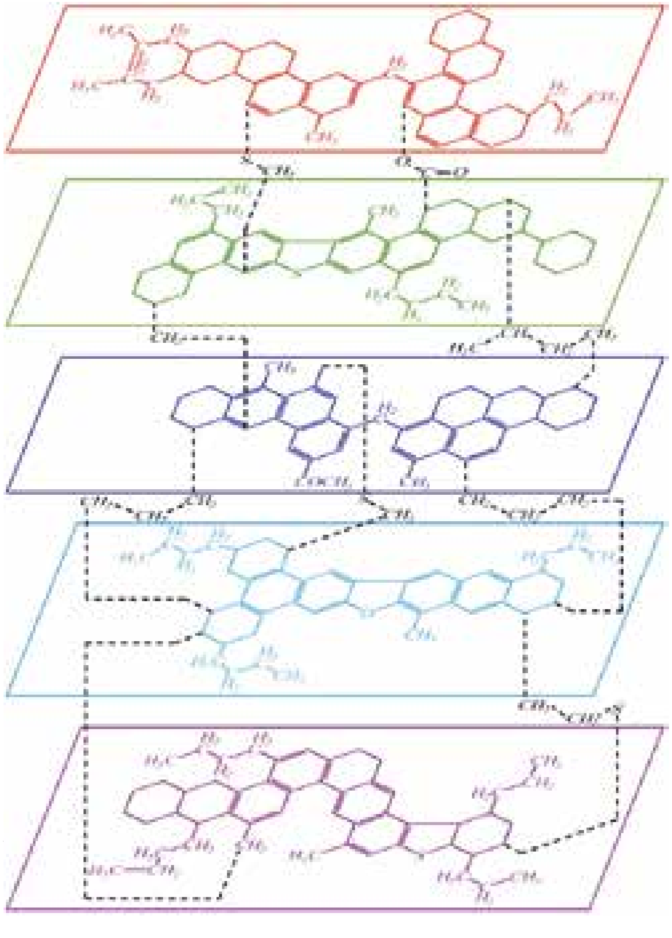

**Fig. 3. Asphaltene molecule model**

**T a b l e 1. Elemental chemical analysis of carbon nanotubes**

| Number | Element content, % | | | | | | | | | | | | |
|---|---|---|---|---|---|---|---|---|---|---|---|---|---|
| | C | O | Al | Si | S | Cl | Ca | Ti | Cr | Mn | Fe | Ni | Cu |
| 1 | 68.61 | 8.35 | 0.1 | 0.17 | 0.01 | – | 0.03 | 0.01 | 0.97 | 0.10 | 0.17 | 18.30 | 0.18 |
| 2 | 67.06 | 6.12 | 0.06 | 0.29 | 0.02 | – | 0.04 | 0.05 | 0.15 | 0.14 | 0.22 | 19.63 | 0.22 |
| 3 | 68.57 | 8.03 | 0.08 | 0.22 | 0.03 | – | 0.01 | 0.05 | 0.23 | 0.12 | 0.16 | 18.82 | 0.19 |

because of their fibrous character, creating a more effective frame. The effectiveness of the technology used to distribute particles uniformly across the volume of the composite matrix determines how much of a reinforcing effect there is.

In terms of strength properties, carbon nanotubes (CNTs) are noticeably superior to most other nanomaterials. They also exhibit exceptional elasticity, allowing them to be bent repeatedly—up to several hundred times—before forming nodes that can fully straighten, restoring the composite to its original form. This property distinguishes CNTs from many other durable materials, which often exhibit brittleness. One approach to modifying the properties of CNTs is the introduction of heteroatoms into their structure, which shows promise for developing new functional and structural materials [26, 27, 28]. Currently, several methods exist for creating modified CNTs. These include filling their internal cavities, adding functional groups to their ends, substituting other elemental atoms for CNT carbon atoms, chemically modifying CNT sidewalls with double bonds, and inserting atoms or molecules into the interstitial spaces of CNT bundles. The choice of precursor depends on factors such as availability, intended operating conditions, its chemical nature (e.g., saturated, or unsaturated hydrocarbons, carbon-to-heteroatom ratio), and the intended application of the nanotubes.

Therefore, the aim of the research was to obtain CNT-bitumen composites, investigate the chemical composition and structure of such composites, and develop composite materials and technological aspects of obtaining carbon-based polymer nanocomposites.

## EXPERIMENTAL PART

### Carbon nanotubes preparation

Saturated ($CH_2Cl_2$, $CH_3CN$, $CS_2$) and unsaturated compounds ($C_2H_2$, $C_7H_8$) were used as carbon precursors and obtained by pyrolytic synthesis. The choice of carbon sources has a significant impact on the temperature of the synthesis, however no direct relationship between the synthesis temperature and the carbon-carbon bond energy of the precursor molecules has been observed. Aluminum oxide membranes were used to compare the characteristics of CNT synthesis and their attributes. The temperature range for obtaining CNTs from acetylene was 700–800°C, toluene 1000–1150°C, dichloromethane 400–600°C, acetonitrile 700–1000°C, a mixture of carbon disulfide and dichloromethane 400–600°C.

Multilayer CNTs were obtained by the catalytic decomposition of propylene (TU U 24.1-03291669-009 standard). The synthesized CNTs had the following parameters: average diameter – 5–170 nm; specific surface area – 200-500 $m^2/h$; bulk density – 15–40 $g/dm^3$; mineral residue content: crude – 6–32.25 wt%, purified – <1 wt%; loss temperature of 5% of the mass after purification of mineral impurities – 520–620°C; specific electrical resistance of compressed powder of nanotubes purified from mineral impurities – 0.05–0.15 Ohms.

The CNT characteristics were determined by the following methods: transmission electron microscopy (JEOL-100CX-II, JEOL, Tokyo, Japan), X-ray diffraction (DRON-3M, Burevestnik, Russia; $\lambda_{Co}$ = 0.179 nm), Raman spectroscopy (Brucker RFS 100/s, Bruker, Billerica, MA, USA), differential thermal and gravimetric analysis (Q 1500 derivatograph, Paulik-Erdey, Hungary; heating rate 10 K/min).

The elemental chemical composition showed that the nanotubes also contained minor impurities of other elements (Table 1).

### Obtaining of the granite crushing

Granite crushed stone was utilized as a coarse aggregate in the manufacturing of asphalt concrete, according to DSTU B V.2.7-75-98 standard. For building materials, goods, structures, and works, crushed stone and thick natural gravel are used [29]. The quality indicators of sand from granite crushing screenings are presented in Table 2, while mechanical and physical indicators of these materials are presented in Table 3.

### Bitumen preparation

Non-activated mineral powder MP-1 from sedimentary rocks was used as a mineral disperse filler. Petroleum road bitumen of BND 90/130 grade was used for the preparation of SDS. Bitumen was studied for compliance with the requirements of DSTU 4044:2019 [30]. Carbon nanotubes (CNTs) were used as a modifying additive of the polymer-bitumen binder.

It was determined to disperse the CNT mixture in the polymer using a specialized dispersing apparatus to achieve a homogenous mixture with uniformly distributed nanotubes for a more uniform dispersion of CNTs in bitumen. The prepared mixture of CNT and polymer was

**Table 2. Indicators of sand properties from granite crushing screenings**

| Parameter | DSTU B V.2.7-32-95 regulations | Value |
|---|---|---|
| Fineness modulus | 2–3 | 2.87 |
| Total residue on a 0.63 mm sieve, wt% | 45–65 | 61.4 |
| Content of powder-like and clayey particles, wt% | Max. 10 | 0.3 |
| Content of clay in lumps, wt% | ≤2 | 0.02 |
| Grade of initial crushed stone in terms of strength | ≥1000 | 1200 |
| Frost resistance grade of the initial crushed stone | – | F300 |

**Table 3. Indicators of granite crushed stone properties**

| Parameter | DSTU B V.2.7-75-98 requirements | Value |
|---|---|---|
| Grain composition. Total residues on sieves, wt% | | |
| D) 5 | 90–100 | 96.1 |
| 0.5 (d + D) | 30–60 | 59.6 |
| D 20. | <10 | 7.5 |
| 1.25 D (25) | <0.5 | 0.38 |
| Content of lamellar and needle-shaped grains, wt% | 15–25 | 23.0 |
| Content of powder-like and clayey particles, wt% | <1 | 0.41 |
| Content of clay in lumps, wt% | NMT 0.25 | Not available |
| Crushed stone grade by crushing capacity | 600–1400 | 1200 |
| Frost resistance | F15–F300 | F300 |
| Bulk density, kg/m$^3$ | – | 1340 |

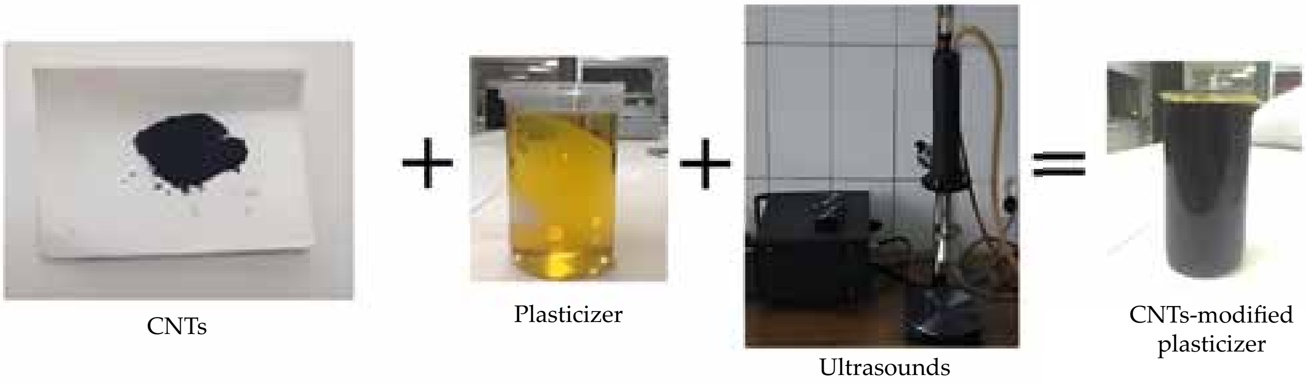

**Fig. 4. Scheme of modified plasticizer preparation (laboratory scale)**

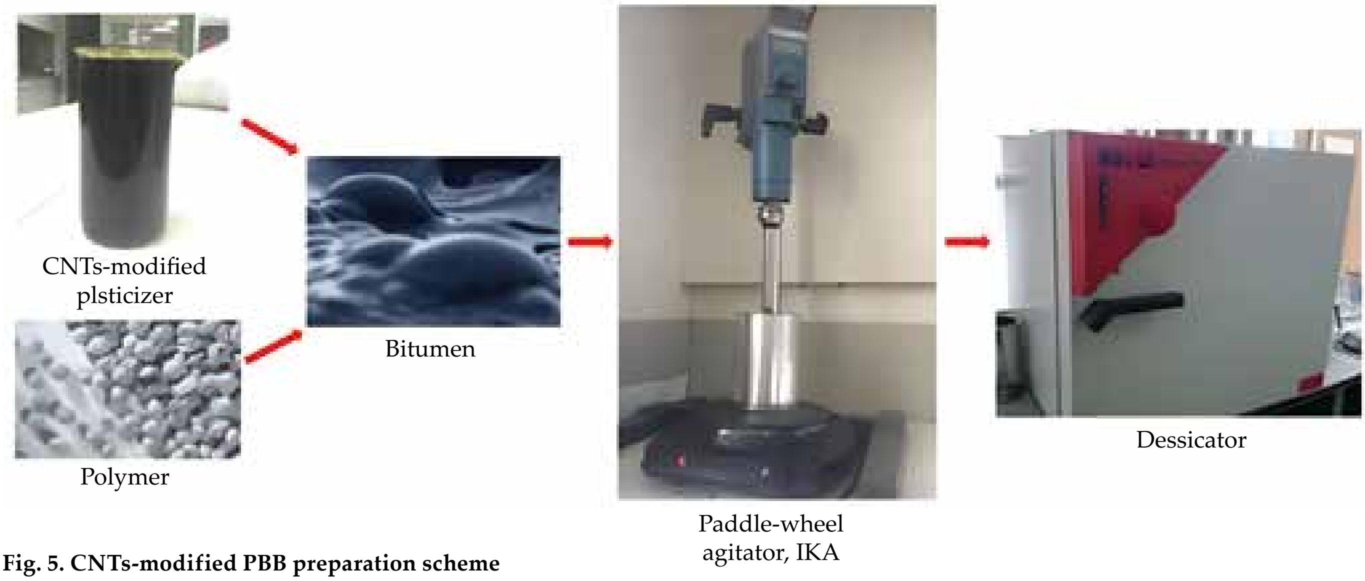

**Fig. 5. CNTs-modified PBB preparation scheme**

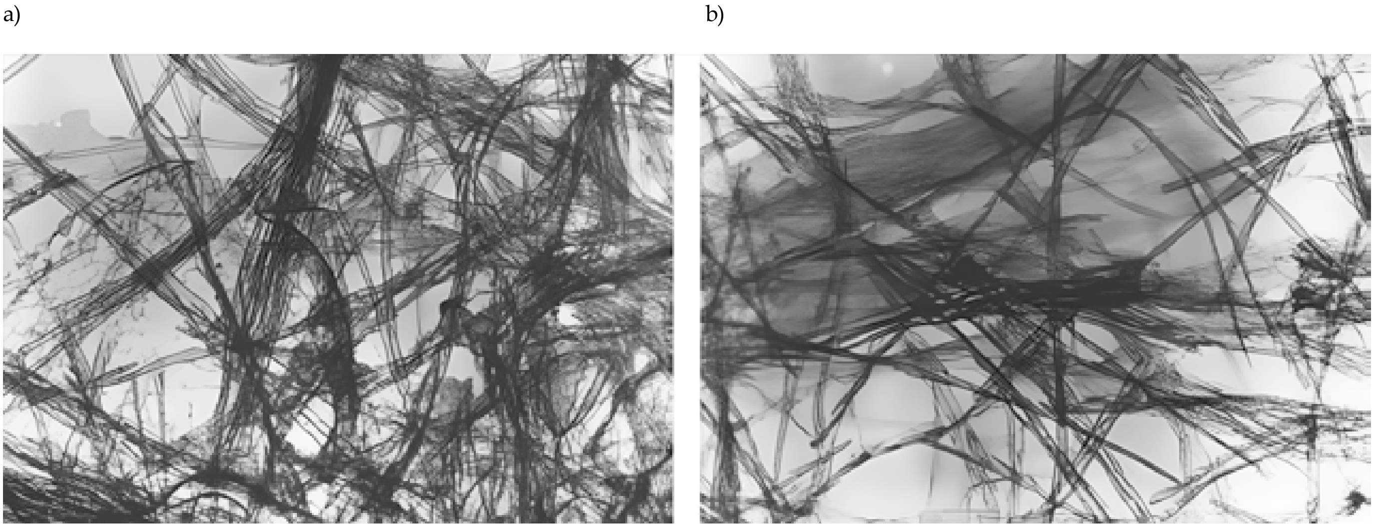

**Fig. 6. TEM images of CNTs at different magnification: a) 48 000×, b) 72 000×**

introduced into the bitumen heated to the operating temperature. The composition was stirred to a homogeneous state for 1.5 hours on an IP-2 type laboratory stirrer. The final formation of the structure of the prepared polymer-bitumen binder with carbon nanotubes occurs within 1.5 hours after the final mixing (Fig. 4 and 5).

It has been established that the cohesive strength of PBB (polymer-bitumen binder) samples, with the introduction of CNTs, increases on average by two times compared to classical samples. CNT gives the highest cohesive strength. In addition, with the introduction of CNTs, a pattern was revealed that was not observed during the tests of basic and reference PBB samples, which consists in restoring the original form - the "self-healing effect" of nanomodified PBB, after determining the cohesive strength.

The observed effect results from the high ability of CNTs to structure the volume of the polymer matrix of the binder, which leads to increased intermolecular interactions and confirms the assumption about the strengthening of the WSP structure and an increased ability of nanomodified binders to reversible deformation.

## RESULTS

The use of the $CH_2Cl_2$ precursor was successful in lowering the temperature of CNT formation (by 250°C compared to acetylene). The morphological characteristics of the CNTs are presented in the TEM images (Fig. 6).

Oxygen-containing functional groups, absorption bands of C-N and C-S bonds are observed in the IR spectra of nitrogen- and sulfur-modified CNTs. According to thermal desorption mass spectrometry, the temperature intervals for the release of CO and $CO_2$ from samples of modified carbon nanotubes are observed in the same range, which may indicate a similar structure of the surface of nanotubes synthesized by the template method.

X-ray fractional analysis showed that the bulk of the nanotubes consist of carbon with a small impurity of nickel (Figure 7).

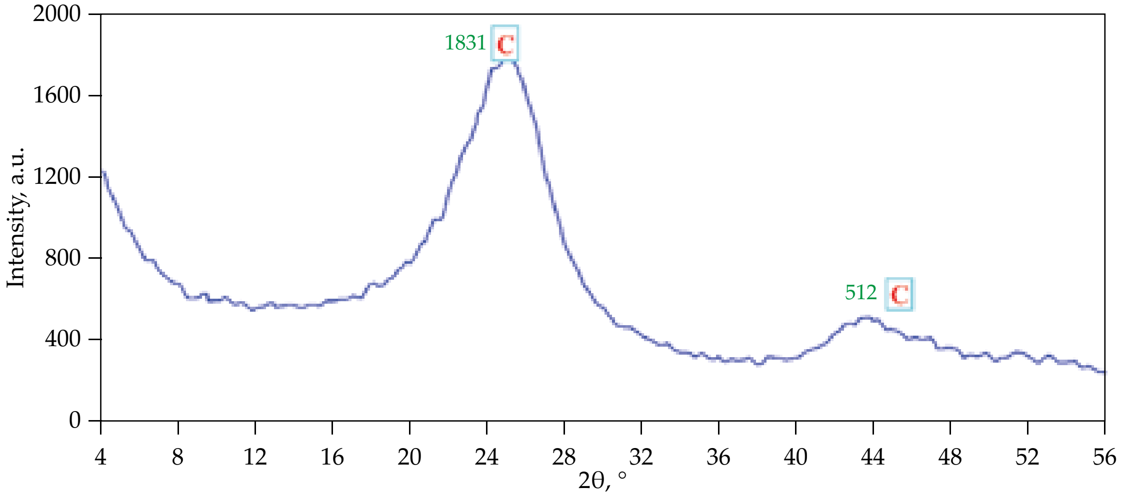

**Fig. 7. X-ray diffraction pattern of CNTs**

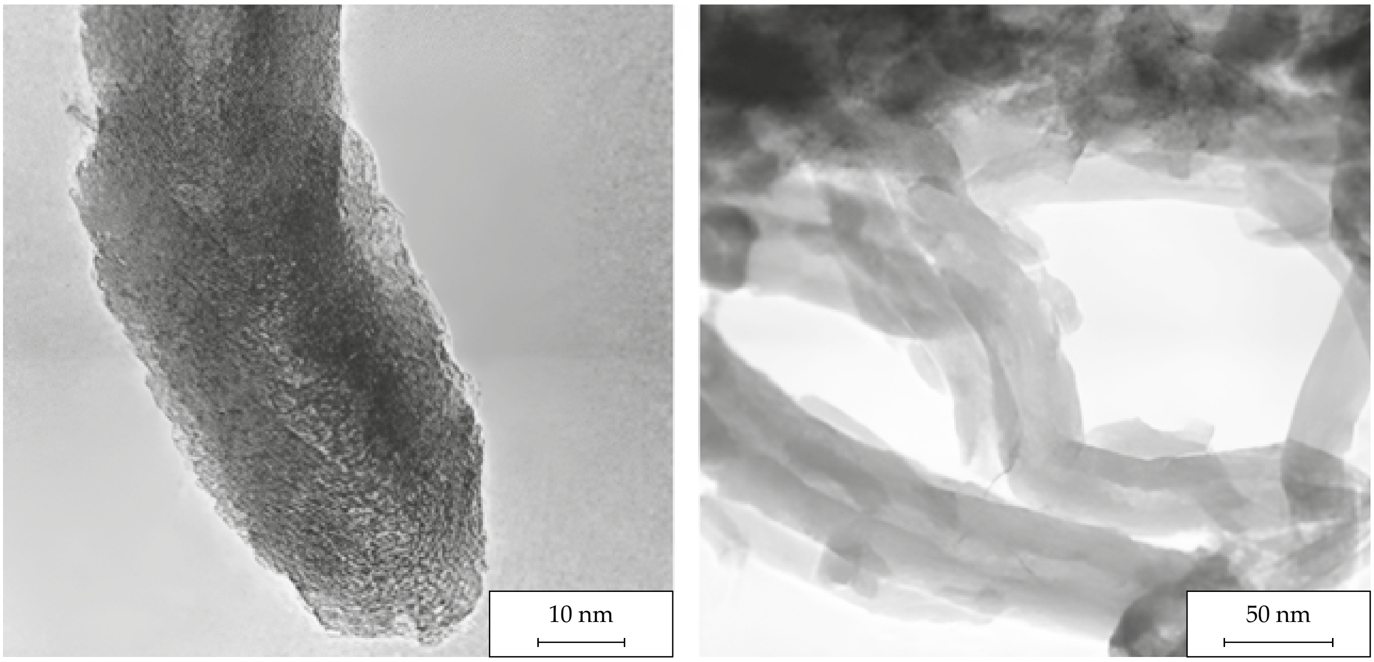

**Fig. 8. TEM images of CNTs at different magnification**

The analysis of the table data showed that in nanotubes the content of particles of various elements is about 32.25%, the bulk of which is represented by Ni (up to 20%). Such content of particles can have a positive effect on the adhesion properties with binders. The insignificant content of chlorine, nitrogen, sulfur in CNT synthesized by the matrix method does not significantly affect their thermal resistance. An important characteristic of carbon materials is the amount of chemisorbed oxygen.

The difference between the results of experiments on temperature-programmed desorption by mass-spectrometric control of samples was the formation of volatile compounds in the first case and the absence of any gaseous chlorine-containing molecules in the second. The maximum temperature of CO and $CO_2$ release for these

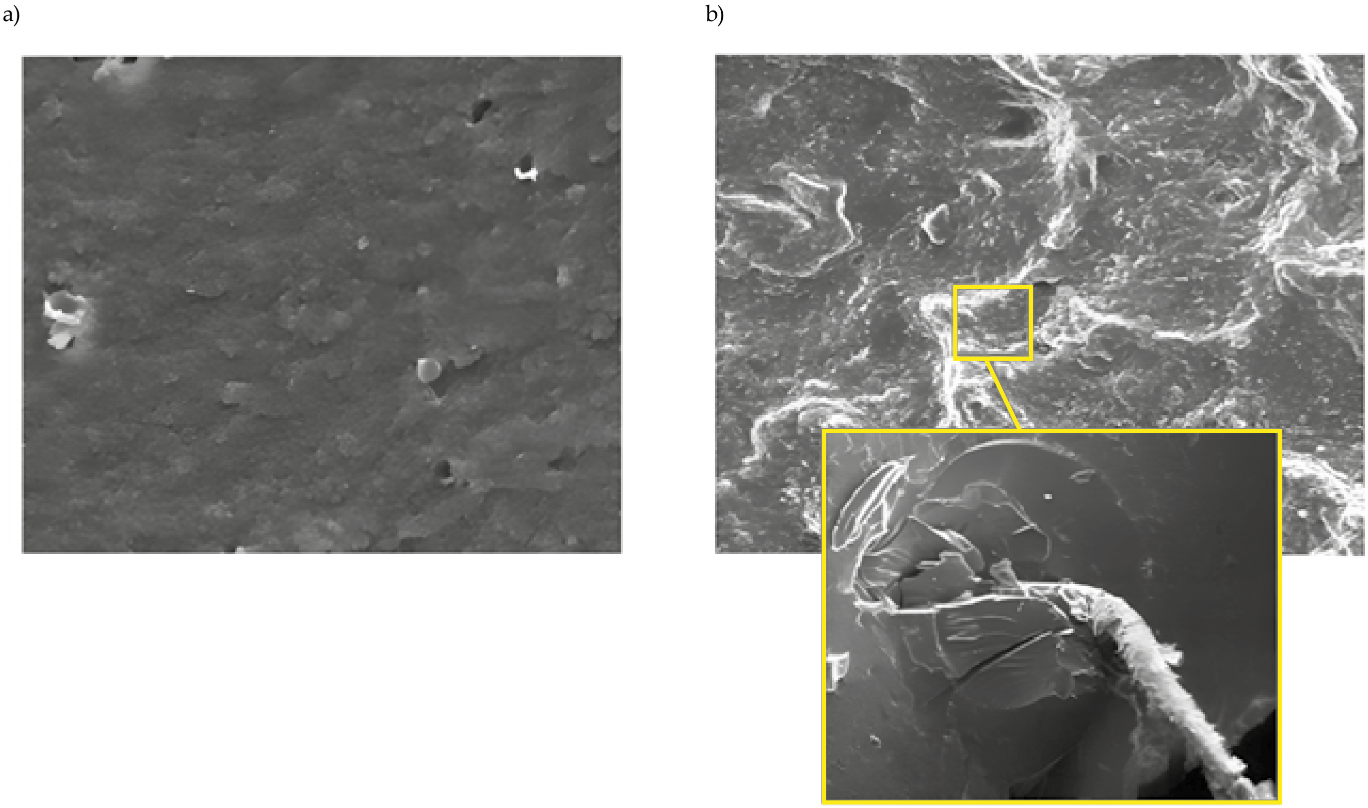

**Fig. 9. SEM images of asphaltene-resin complexes structure: a) PBB, b) PBB/CNTs**

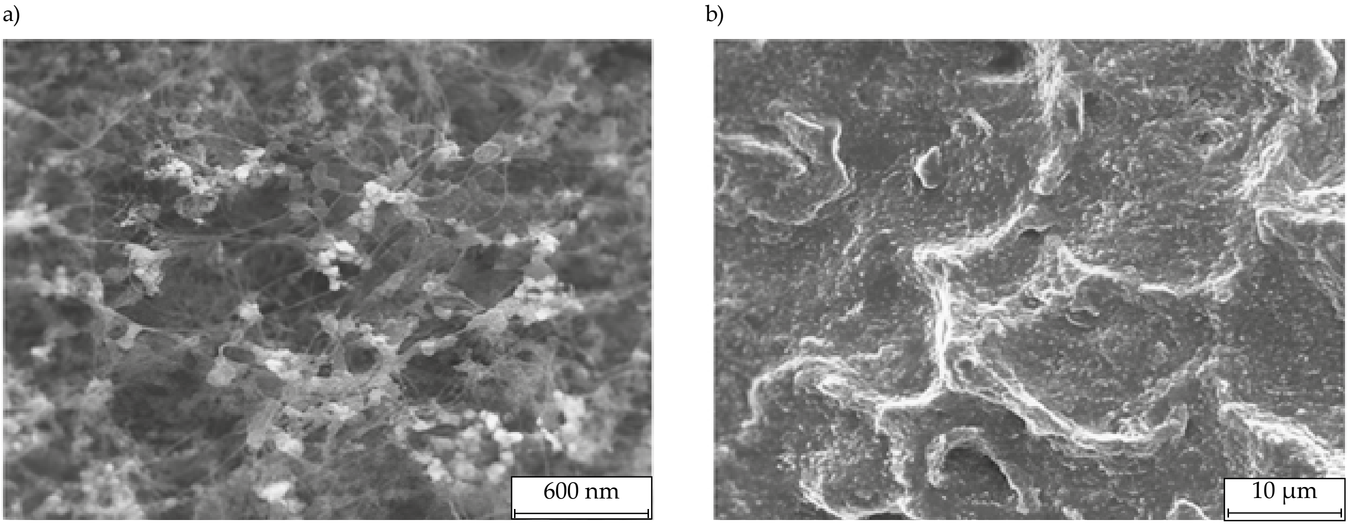

**Fig. 10. SEM images: a) CNTs, b) ARC with CNT**

samples are observed in the same range. In the case of $CO_2$ desorption from different samples, the ratio of low and high temperature peaks is slightly different. The CO and $CO_2$ emission limits are like those observed for activated carbon (Fig. 8).

TEM images of CNTs (Fig. 8) showed that carbon particles are intertwined in bundles and are sizes from 5 to 170 nm, and their length can reach up to 250 nm. Nanotubes have uneven and damaged outer layers, which should improve the adhesive bond with the matrix material. They are bent and intertwined, which leads to the formation of nanotube beams/aggregates.

Scientists believe that asphaltenes, or as they are known, according to recent studies, asphaltene-resin complexes (ARC), are one of the most significant structural-forming constituents of both oils and bitumen's. Asphaltenes are high-molecular hydrocarbons characterized by a clustered molecular structure, polarity, paramagnetism and a high tendency to intermolecular interactions and associations. It is proved that CNTs have chemical affinity with ARC, which function as "molecular Velcro", which will ensure their active interaction with each other. In this regard, it was assumed that the study of the dynamics of changes in the parameters and structure of ARC under the influence of CNTs will allow structural changes in the volume of PBB [31, 32]. The mechanism of CNT influence on the PBB structure was investigated by electron microscopy. Asphaltene-resin complexes (ARC) from the polymer-bitumen binders were studied (Fig. 9).

As can be seen in Fig. 9a, the structure of PBB is homogeneous, granular, and consists of large asphaltene-resin complexes that resemble clusters. Asphaltene-resin complexes have a nanotube structure after the introduction of CNTs (Fig. 9b). At the same time, structural elements are formed from CNTs that prevent ARC coagulation. Their dispersion increases, which slows down the aging processes and minimizes the PBB stratification processes. The resulting filamentary formations are confirmation that carbon nanomaterial's structure polymer-bitumen binders with preservation of elastic-elastic properties, which correlates with the data on increased cohesive strength and elasticity of modified SDS. The capacity of the latter to "adapt to the environment" was observed while examining the SEM images of the original CNTs and ARCs from the investigated nanomodified PBB (Fig. 10).

Micrograph analysis allows us to establish that the shape and dispersion of carbon nanomaterials influence the structure of ARC. The addition of CNTs, which initially have a fibrous structure, causes them to penetrate asphaltene-resin complexes and increase their dispersion. At the same time, the formation of structures that prevent coagulation of asphaltene-resin complexes is observed.

The change in the linear dimensions of ARC before and after modification was investigated to evaluate the impact of CNTs on the processes of PBB structure creation. As a result, the addition of CNTs causes the average ARC particle size to drop by 30% in the range of up to 0.8 μm, increasing viscosity, decreasing delamination, and enhancing the durability of the characteristics of nanomodified PBBs. Summarizing the results obtained in the study of the parameters and structure of ARC, we can formulate the following mechanism for the structuring processes of polymer-bitumen binder modified with carbon nanotubes:

– when combining bitumen and carbon nanotubes, they penetrate into asphaltene-resin complexes, with a subsequent increase in ARC dispersion, the average size of ARC blocks in the range of up to 0.8 μm decreases by 30% for CNT-modified PBB;

– the consequence of the ongoing processes is the formation of structural elements that prevent the coagulation of asphaltene-resin complexes with each other;

– with the subsequent combination of the system with the polymer, a strengthened spatial structural grid is formed, with the additional formation of stable bonds with a polymer matrix with dispersed asphaltene-resin complexes.

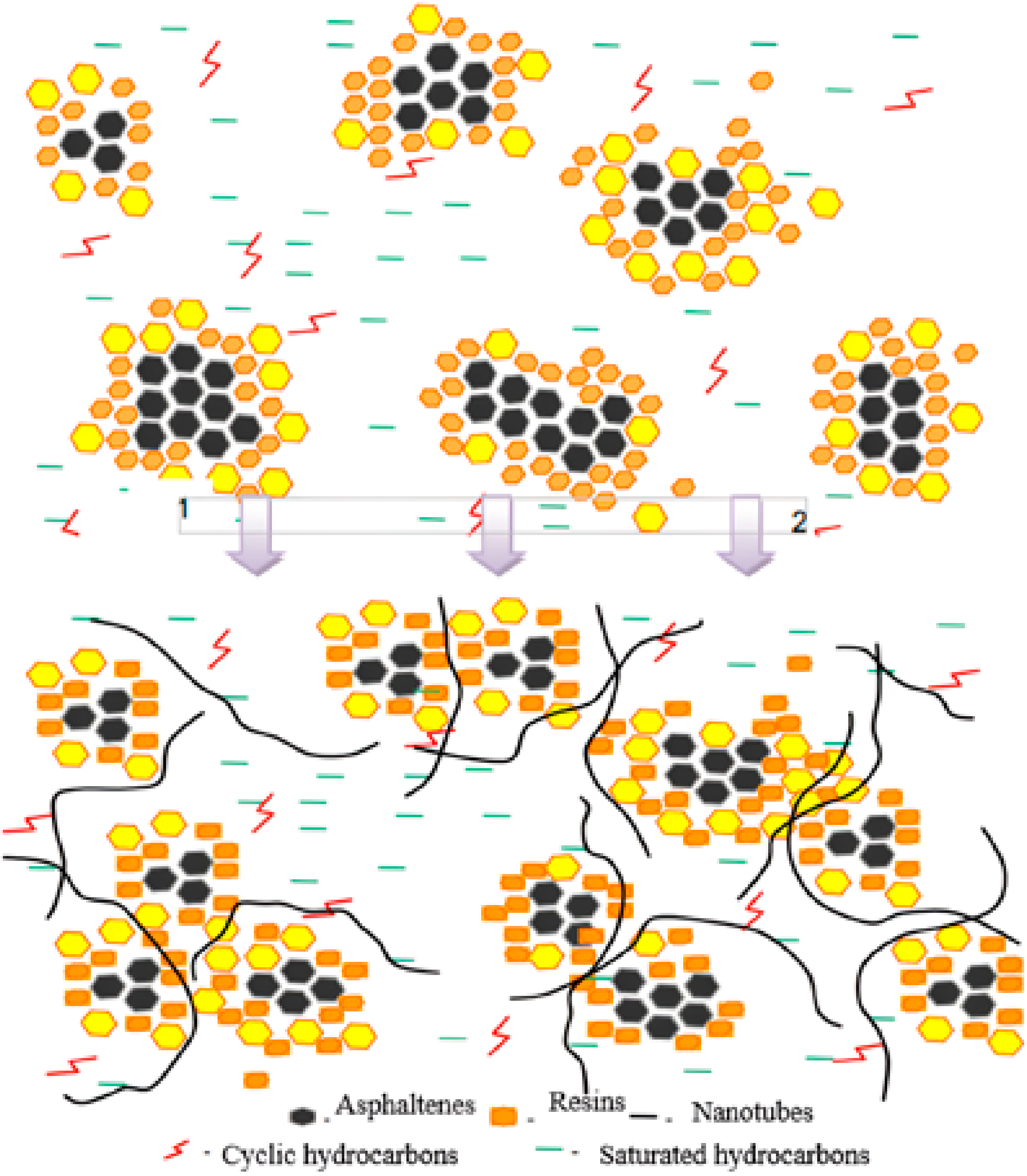

**Fig. 11. Schematic diagram of CNTs-modified PBB structure**

The schematic diagram of CNTs-modified PBB structure is shown in Fig. 11.

Carbon nanotubes function as a kind of obstacle in the coagulation of asphaltene-resin complexes, which tend to self-assemble, resulting in the aggregation of ARC. This cause instability of the dispersed system and deterioration of the binder's quality, as demonstrated by electron microscopy photographs (Fig. 12).

The introduction of the polymer into the system leads to the formation of a reinforced spatial structural grid (Fig. 13), which positively affects the structure's ability to perceive the effects of external factors.

The emergence of spatial structures (that is, the transition from a free to a coherently dispersed state) radically changes the structural and mechanical properties of the system. It becomes completely sediment-resistant, since the presence of a structural reinforced polymer mesh keeps the particles of the dispersed phase fixed in it from precipitating. At the same time, such systems in operating conditions lose fluidity and mobility. Their viscosity increases continuously with increasing dispersion and a corresponding decrease in particle size and their concentration in dispersion media. Achieving a cohesion-dispersed PBB structure will provide effective shear strain resistance, which will positively affect the quality of asphalt concrete prepared using it.

## DISCUSSION

The use of nanomodified binders in polymer asphalt concrete mixtures provides a significant increase in water resistance and deformative stability of asphalt concrete. Water resistance index for Sample 2 (modified CNT) in an amount of 0.3%, without the use of additional adhesive and cross-linking additives, increases by 20% and 12%, respectively, compared to samples of asphalt concrete based on the control composition (Table 4 and 5).

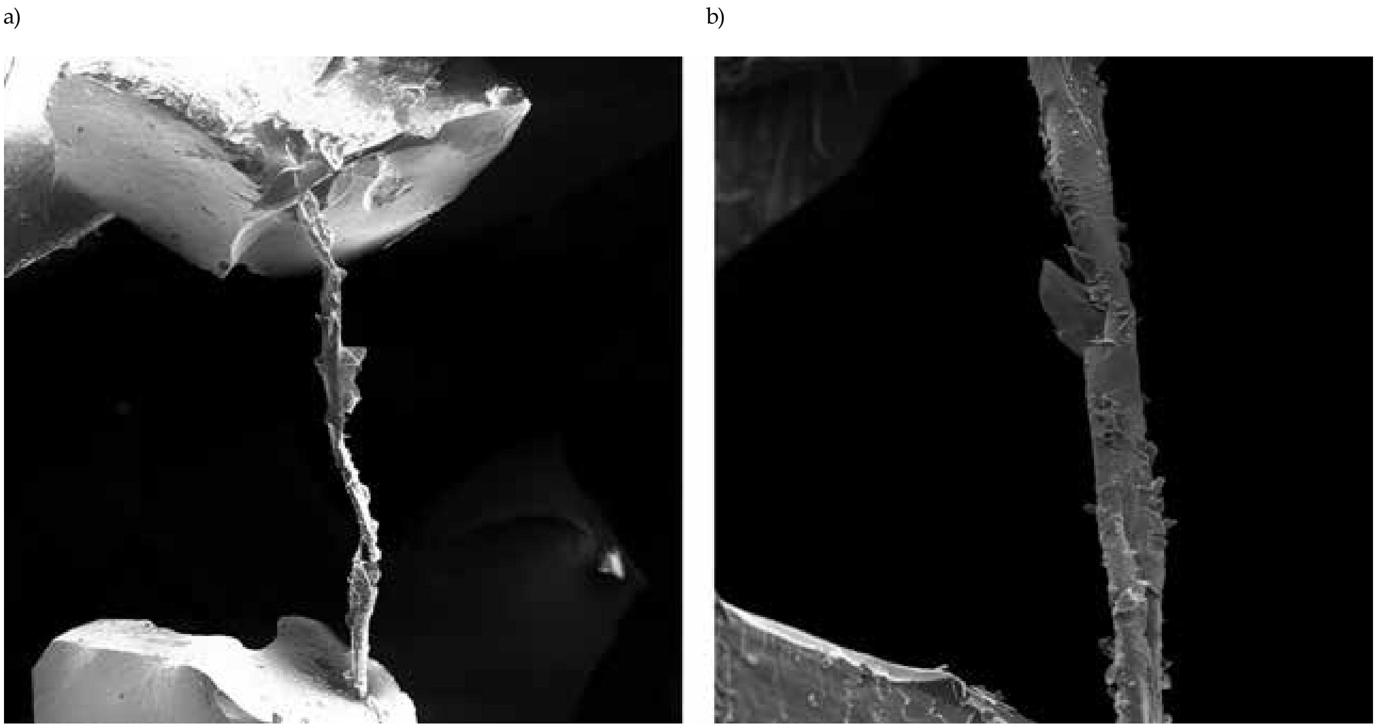

**Fig. 12. SEM images of PBB**

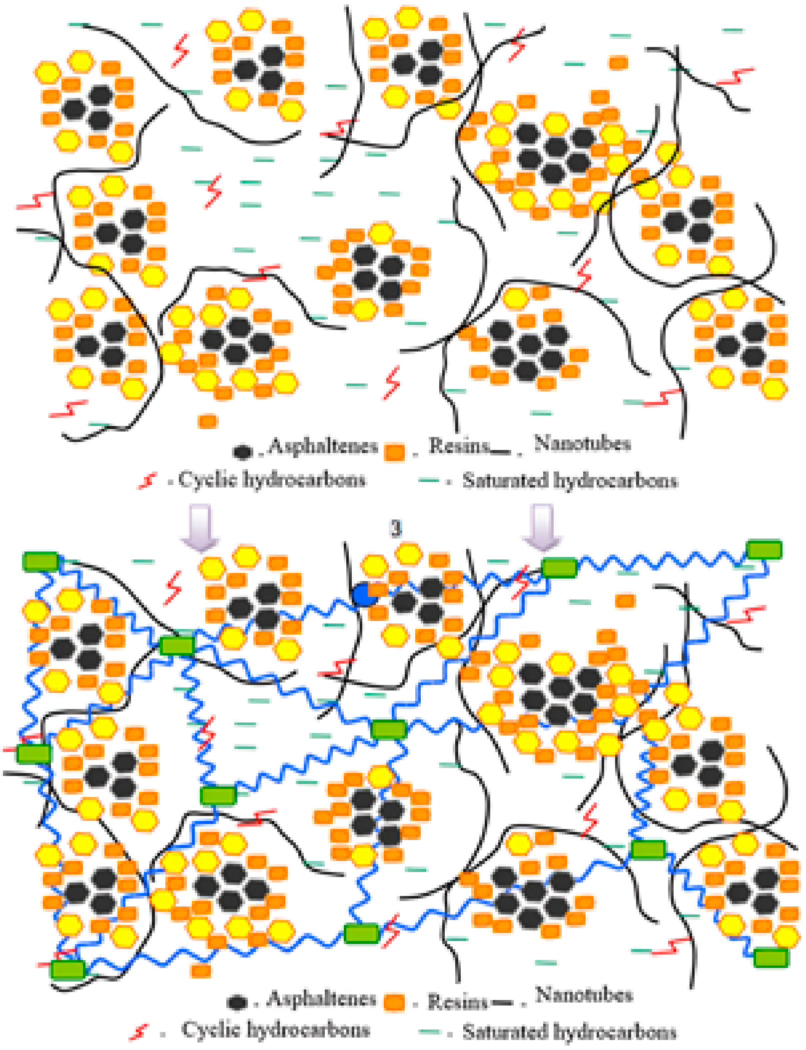

**Fig. 13. Schematic diagram of reinforced CNT-modified PBB spatial network structure**

**Table 4. Compositions of the optimal CNTs-modified polymer-bitumen binder**

| Component | Sample 1 | Sample 2 | Sample 3 |
|---|---|---|---|
| Carbon nanotubes, wt % | 0.1 | 0.3 | 0.5 |
| Polymer, wt% | 3.5 | 2.8 | 2.8 |
| Bitumen BND 90/130, wt% | The rest | | |

The most important property of modified asphalt concrete, which characterizes its durability, is the ability of its structure to effectively resist destruction in conditions of changing humidity and temperature regimes.

Polymer asphalt concrete deteriorates similarly to other building materials, primarily when it is exposed to extended dampness. Long-term exposure to moisture in asphalt concrete pavements can cause water diffusion into a bituminous film, which can then separate from the surface of the mineral grains. This compromises the structural integrity of the pavement, leading to increased coating wear as well as the development of deformations and potholes. Furthermore, water seeps into the structure's microdefects in the asphalt concrete, causing a consistent loss of strength.

The test results presented showed that the obtained composites are characterized by increased physical and mechanical characteristics: compressive strength, shear resistance, water resistance under short-term water exposure. Therefore, it is important to study the stability of the asphalt concrete structure modified by CNTs under prolonged aggressive water exposure. The results of tests of long-term water resistance of asphalt concrete samples are shown in Figure 14.

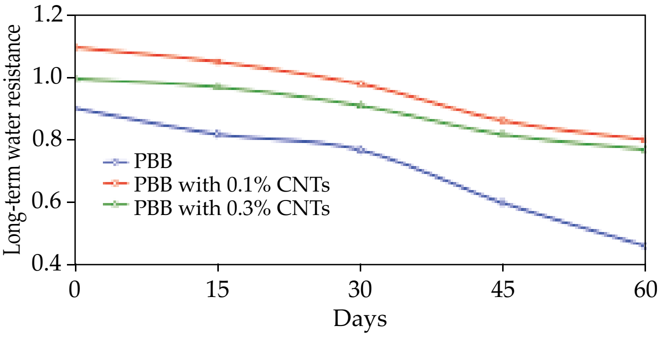

**Fig. 14. Long-term water resistance of asphalt concrete**

Analysis of long-term water resistance data shows that the introduction of nanomodifiers increases the ability of asphalt concrete to resist the destructive effects of water during prolonged water saturation. Since nanomodified PBBs are known for having increased adhesion strength, the indicator of long-term water resistance after 60 days for asphalt concretes prepared based on PBB with CNT in the amount of 0.3 wt% of bitumen is markedly higher than the value of this indicator for asphalt concrete of the control composition. Thus, the resulting nanomodified polymer asphalt concrete has improved resistance to aggressive effects of precipitation and wastewater and is able to provide long-term defect-free durability of the asphalt concrete structure.

Analysis of strength indicators shows that with the introduction of CNTs in the amount of 0.3 wt%, the tensile strength indicators at temperatures of 20°C, 50°C increase by 58% and 54%. Thus, the increase in strength indicators amounted to 53% at temperatures of 20°C and 47% at 50°C. An increase in cohesive strength and the binder's softening temperature, which inevitably results in an increase in the effective resistance to mechanical loads, accounts for the increased strength characteristics of polymer asphalt concrete modified with carbon nanomodifiers. When the mixture is compressed, the mineral backbone particles converge, and the system's internal

**Table 5. Indicators of modified asphalt concrete properties**

| Indicator | Requirements of DSTU B V.2.7-119 | Sample 1 | Sample 2 | Sample 3 |
|---|---|---|---|---|
| Water saturation, % | ≤3.5 | 1.87 | 1.6 | 1.8 |
| Average density, kg/m$^3$ | – | 2.41 | 2.41 | 2.41 |
| Compressive strength, MPa at temperature: | | | | |
| +20°C | ≥2.5 | 254 | 4.02 | 3.90 |
| +50°C | ≥1.3 | 1.94 | 2.95 | 2.80 |
| OS | ≤12.0 | 8.9 | 8.7 | 8.3 |
| Water resistance | ≥0.9 | 0.90 | 1.10 | 1.00 |
| Long-term water resistance | ≥0.85 | 0.85 | 1.05 | 1.00 |
| Ultimate tensile strength (crack resistance) at splitting at 0°C | – | 2.81 | 3.85 | 3.80 |
| Shear resistance according to: | | | | |
| - coefficient of internal friction tgφ; | – | 0.92 | 1.14 | 1.01 |
| - shear cohesion at 50°C | – | 0.61 | 0.97 | 0.86 |

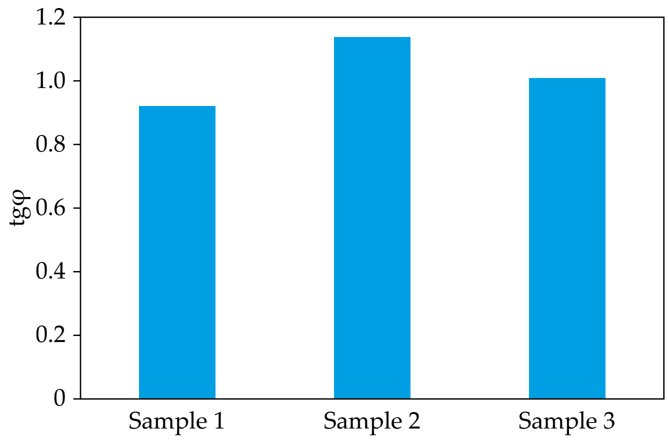

**Fig. 15. Coefficient of internal friction of the samples**

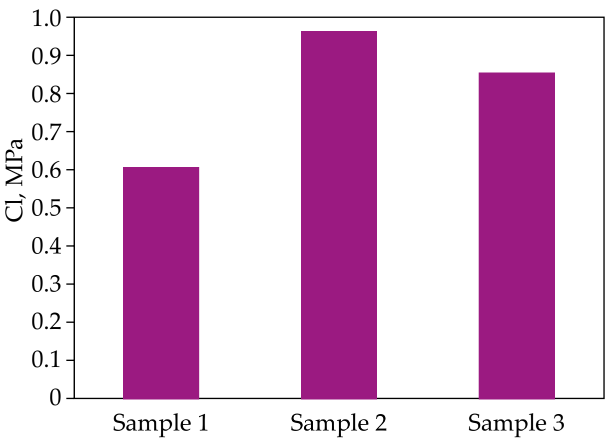

**Fig. 16. Shear adhesion of the samples**

friction rises because of the mineral particles contacting along the adsorption-solvate shells with greater viscosity. Accordingly, the internal friction and jamming of mineral particles in the mixture influence the mechanical strength of asphalt concrete.

The mineral backbone's particle size distribution, density, and, most importantly, the size, shape, and composition of the grain surface determine the forces of internal friction and jamming. Internal adhesion forces increase with an increase in density, particularly when it comes to particle size, roughness, and angularity. The adhesion forces between the binder and the mineral backbone particles are contingent upon the binder's viscosity and its physicochemical interactions with the mineral components. In order to compute the asphalt concrete's coefficient of internal friction and shear resistance, loads were established under various loading schemes that resulted in the destruction of samples, such as cylinders, and the related limiting deformations.

Figures 15 and 16 show the shear resistance of polymer asphalt concrete. The addition of CNTs increases the yield strength, which is related to the elastic component of the shear resistance.

The temperature sensitivity of asphalt concrete is a known drawback, so it is critical that the road composite maintains its strength qualities despite temperature fluctuations. The degree of stability of the strength characteristics of asphalt concrete with a change in temperature in the summer period characterizes the heat resistance coefficient can be calculated using Equation 1:

$$k_T = R_{50}/R_{20} \tag{1}$$

Fig. 17 shows that the introduction of CNT leads to an increase in the thermal resistance coefficient. Thus, the use of CNT in the amount of 0.3 wt.% (Sample 2) allows to increase the thermal resistance coefficient of polymer asphalt concrete, in comparison with the base composition, by 28%.

The parameter characterizing the degree of stability of the properties of polymer asphalt concrete at differences from positive temperatures to negative ones is the crack resistance coefficient, which is calculated as the ratio of the compressive strength at a temperature of 50 °C to the compressive strength at a temperature of:

$$0°\mathrm{C} - k_f = R_{50}/R_0 \tag{2}$$

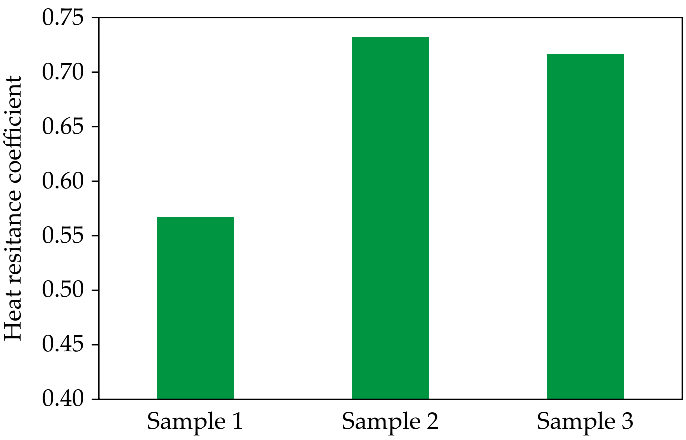

**Fig. 17. Heat resistance coefficient of the samples**

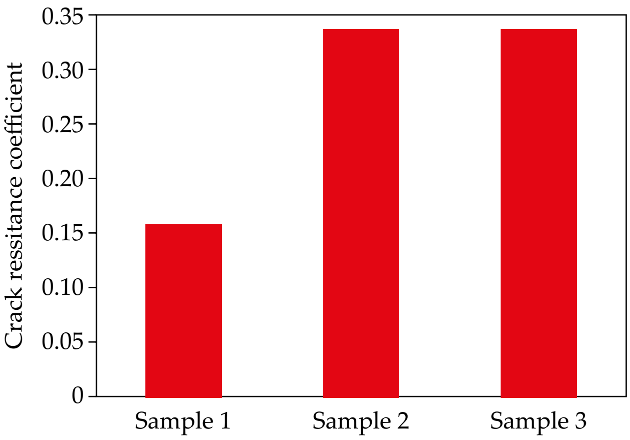

**Fig. 18. Crack resistance coefficient of the samples**

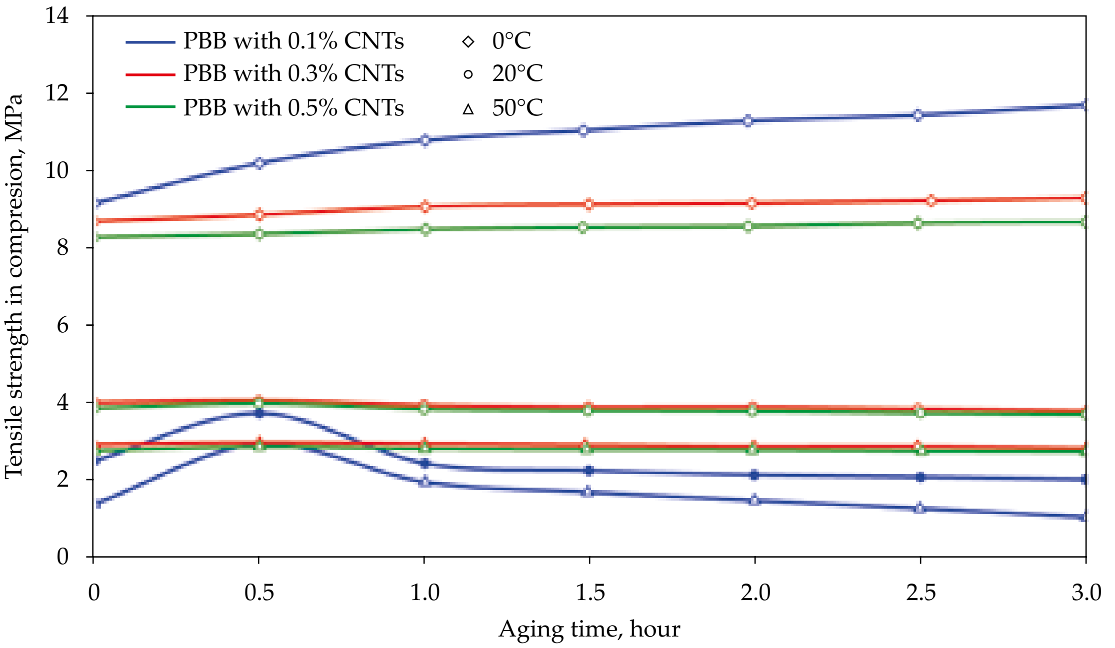

**Fig. 19. Effect of aging on tensile strength of asphalt concrete**

Fig. 18 shows that with the introduction of CNTs into the composition of polymer-asphalt concrete, the crack resistance coefficient increases twice.

Therefore, it is possible to form a strong, waterproof, and temperature-resistant layer of a structured nanomodified binder on the surface of a stone material by controlling the structure formation of asphalt concrete during the initial stage of PBB preparation by introducing a nanomodifier. This naturally endows the material with a useful set of properties.

The operational reliability and durability of asphalt concrete is due to the speed of the aging processes of the binder. The aging processes of asphalt concrete during preparation are several times more intense than during the operating period. Therefore, to establish the effect of CNTs in the composition of PBB on the aging intensity of asphalt concrete, the physical and mechanical characteristics of asphalt concrete samples were studied, which were prepared from aged, at a temperature of approx. 150°C for 0.5, 1, and 3 hours.

The intensity of the ongoing oxidation processes was assessed by increasing the strength properties of asphalt concrete samples at different test temperatures and changing the water resistance. The test results presented in Fig. 19 indicate that samples of asphalt concrete prepared based on CNT-modified PBB are characterized by increased strength indicators, both before aging and after. However, the dynamics of changes in strength indicators during the aging process is much lower than in the case of using PBB of the basic composition. Thus, when using PBB of the basic composition, it was found that the strength of asphalt concrete at 20°C after 3 hours of heating the mixture decreased by 20%, and with PBB with CNT by 4%. The compressive strength at 50°C changed by 23.3 and 3%, respectively.

Strength indicators at 0°C show that CNTs have a major impact on the characteristics of asphalt concrete. Fig. 19 illustrates the mildly curved curve that represents the variations in the composite's strength with CNT-modified PBB. Following three hours of mixture thermosetting, the indicator increased by 6.5% and 4.5%, respectively. After three hours of warming up, tensile strength increases by more than 27%, indicating that the dynamics of changes in the strength of asphalt concrete, manufactured using PBB of the basic composition, occur more intensely. The obtained results testify to the effective counteraction of CNTs in the composition of the PBB to the structural changes occurring during the aging process, which will positively affect the durability of the asphalt concrete pavement.

The ability of asphalt concrete to resist deformation and fracture is due to its structure and depends on rheological properties such as viscosity, elasticity and ductility related to the fatigue strength and durability of the material. The most important indicators that determine the shear resistance of asphalt concrete in the pavement also include track resistance.

The determination of the rut resistance of nanomodified polymer asphalt concrete was examined. Samples of type B asphalt concrete slabs with the same amount of binder were created for this purpose. The main goal of the approach is to determine the track depth on an asphalt concrete slab that has been constructed by repeatedly moving a wheel in a car-simulating manner while subjected to a specified vertical force and 60◎of test temperature. The obtained results of measuring the track depth are shown in Fig. 20.

It has been established that polymer asphalt concrete, based on nanomodified PBB, is more resistant to the formation of a rut than polymer asphalt concrete of tradi-

**T a b l e 6. Indicators of physical, mechanical, and operational properties of polymer asphalt concrete type B**

| Indicator | Requirements of DSTU B V.2.7-119 | Sample 1 | Sample 2 | Sample 3 |
|---|---|---|---|---|
| Physical and mechanical properties | | | | |
| Compressive strength, MPa at temperature: | | | | |
| +20°C | ≥2.9 | 254 | 4.02 | 3.90 |
| +50°C | ≥1.3 | 1.94 | 2.95 | 2.80 |
| 0°C | ≥8.0 | 8.9 | 8.7 | 8.3 |
| Ultimate tensile strength (crack resistance) at splitting at 0°C | – | 2.81 | 3.85 | 3.80 |
| Shear resistance according to: | | | | |
| – coefficient of internal friction tgφ; | – | 0.92 | 1.14 | 1.01 |
| – shear cohesion at 50°C | – | 0.61 | 0.97 | 0.86 |
| Track depth (20,000) cycles | – | 11.5 | 4.6 | 3.8 |
| Fatigue life (at $T$ = 10°C), cycle | – | 200,000 | 410,000 | 460,000 |
| Water resistance | 0.9 | 0.9 | 1.10 | 1.00 |
| Long-term water resistance | 0.85 | 0.85 | 1.05 | 0.97 |

tional composition. The gauge depth after 20,000 passes on samples of polymer asphalt concrete on PBB modified by CNT with both 0.3 wt% and 0.5 wt% is 2.5 and 3 times, respectively, less than on samples of asphalt concrete without CNTs (Fig. 21).

Since the tests were conducted at a temperature of 60°C, in an aqueous medium, the results obtained characterize the resistance of asphalt concrete on the studied binders to shear loads (shear resistance) and moisture. The shear resistance of asphalt concrete is determined by the static and dynamic yield strengths, the latter being due to the coagulation structure of bituminous films. Comparison of the cohesive strength of the PBB samples and the data obtained in the study of the gauge on the surface of asphalt concrete slabs allows us to conclude that during the preparation and compaction of the asphalt concrete mixture, a strong, temperature-resistant and waterproof layer of a structured nanomodified binder is formed on the surface of the grains of the mineral material. Obviously, this contributes to a change in the yield strength of asphalt concrete above the level of maximum tangential stresses, which leads to a slight accumulation of residual plastic deformations in the coating. To obtain a complete assessment, a comparison of the physical-mechanical and performance properties was conducted, which are shown in Table 6.

The quality of the developed nanomodified polymer asphalt concrete was assessed by the following indicators of physical and mechanical properties: water saturation, compressive strength at temperatures 0°C, 20°C, 50°C,

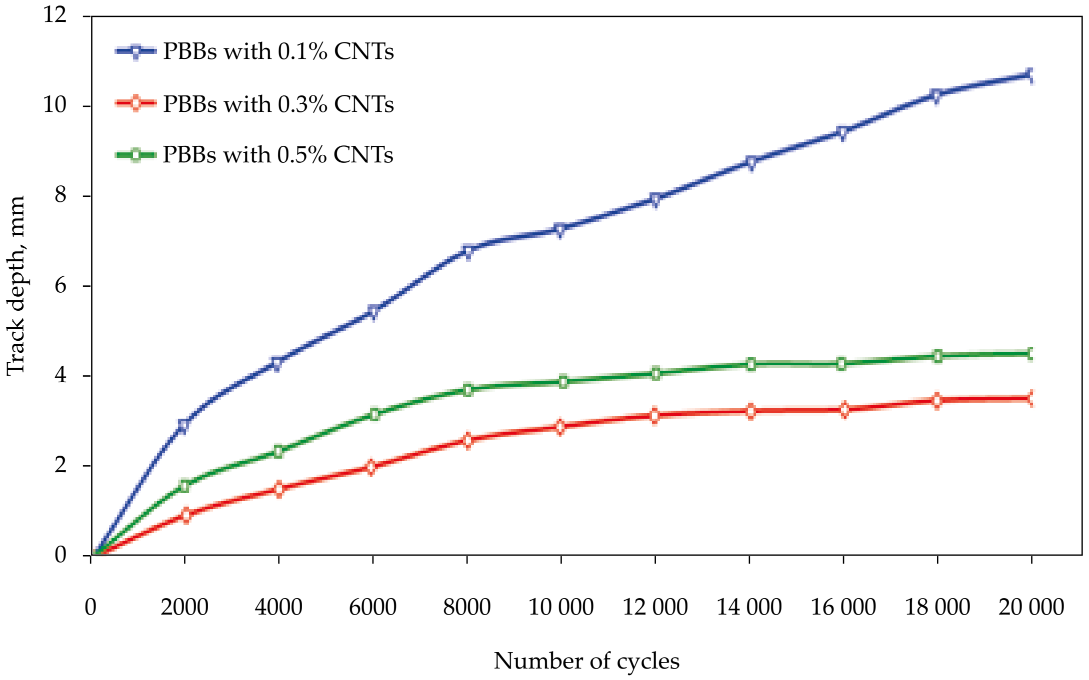

**Fig. 20. Depth of asphalt concrete trace depending on the number of cycles**

**Fig. 21. View of the slab after 20,000-wheel passes: a) PBB with 0.3 wt.% CNT and PBB with 0.5 wt.% CNT, b) PBB with 0.1 wt.% CNT**

**Table 7. Quality criteria for CNT-modified polymer asphalt concrete**

| Indicator | Equation | Note |
|---|---|---|
| | Physical and mechanical properties | |
| Strength criterion | $k_{Rcom\,20} = \frac{R'_{com\,20}}{R_{com\,20}}$ | $R_{com20}$ and $R'_{com20}$ is the compressive strength at a temperature of 20°C of nanomodified and traditional asphalt concrete, respectively, MPa |
| High-temperature strength criterion | $k_{Rcom\,50} = \frac{R'_{com\,50}}{R_{com\,50}}$ | $R_{com50}$ and $R'_{com50}$ is the compressive strength at a temperature of 50°C of nanomodified and traditional asphalt concrete, respectively, MPa |
| Low-temperature strength criterion | $k_{R0} = \frac{R'_{com\,0} \cdot k'_{split}}{k_{split}}$ | $k_{Rcom0} = R'_{com0}/R_{com0}$, where $R_{com0}$ and $R'_{com0}$ are the compressive strength at a temperature of 0°C of nanomodified and traditional polymer asphalt concrete, respectively, MPa; $k'_{split} = \frac{R^{DSTU}_{split} - R'_{split}}{R^{DSTU}_{split}}$ and $k_{split} = \frac{R^{DSTU}_{split} - R_{split}}{R^{DSTU}_{split}}$, where $R'_{pack}$ and $R_{split}$ are the tensile strength at splitting at a temperature of 0°C of nanomodified and traditional polymer asphalt concrete, respectively, MPa. – the optimal value of the tensile strength with a split at a temperature of 0°C, adopted 4.4 MPa (the middle of the permissible interval from 2.8 to 6.0 MPa) |
| Shear resistance criterion | $k_{sr} = \frac{C'_l \cdot tg'(\varphi)}{C_l \cdot tg(\varphi)}$ | $C'_l$ and $C_l$ is the laboratory cohesion index for shear of nanomodified and traditional polymer asphalt concrete, respectively, MPa.<br>and are the coefficient of internal friction of nanomodified and traditional polymer asphalt concrete, respectively. |
| | Performance | |
| Water resistance criterion | $k_{watr} = \frac{k'_B \cdot k'_{watr}}{k_B \cdot k_{watr}}$ | and is the coefficient of nanomodified and traditional polymer asphalt concrete, respectively.<br>and is the resistance coefficient after prolonged water saturation of nanomodified and traditional polymer asphalt concrete, respectively |
| Rutting resistance criterion | $k_C = \frac{h_k}{h'_k}$ | and is the gauge depth after 20,000 passes of the wheel for samples made of nanomodified and traditional polymer asphalt concrete, respectively, mm. |
| Durability criterion | $k_{dur} = \frac{D'_f}{D_f}$ | and is the fatigue durability at a temperature of 10°C of samples from nanomodified and traditional polymer asphalt concrete, respectively, the cycle. |

heat resistance coefficient, crack resistance coefficient, tensile strength at splitting at temperatures 0°C, internal friction coefficient, shear cohesion at a temperature of 50°C, as well as performance indicators: resistance to rutting, fatigue durability, water resistance and long-term water resistance. The developed partial quality criteria for nanomodified polymer asphalt concrete were calculated in accordance with the formulas given in Table 7 and 8.

In evaluating the efficacy of incorporating carbon nanomodifiers into the polymer-bitumen binder to pro-

**T a b l e 8. Partial calculation of quality criteria for CNT- modified asphalt concrete**

| Criteria description | Partial criterion value | | |
|---|---|---|---|
| | Sample 1 | Sample 2 | Sample 3 |
| Physical and mechanical properties | | | |
| Strength | 1.00 | 1.58 | 1.54 |
| High-temperature strength | 1.00 | 2.05 | 1.94 |
| Low-temperature strength | 1.00 | 1.37 | 1.35 |
| Shear resistance | 1.00 | 1.97 | 1.55 |
| Performance | | | |
| Water resistance | 1.00 | 1.51 | 1.31 |
| Rutting resistance | 1.00 | 2.50 | 3.03 |
| Durability | 1.00 | 2.05 | 2.30 |

duce asphalt concretes, a comprehensive quality criterion was computed. This criterion considers developed partial quality criteria and employs diverse weighting coefficients, as indicated by the Equation 3 and 4:

$$F_C = \alpha_1 K_{pm} + \alpha_1 K_{\text{oper}} \qquad (3)$$

where  - weight coefficients.

$$k_{pm} = \sqrt[4]{k_{R\,com\,20} \cdot k_{R\,com\,50} \cdot k_{R\,0} \cdot k_{sr}} \qquad (4)$$

where $K_{pm}$ *is* the criterion of physical and mechanical properties characterizing the tensile strength at different temperatures (50, 20 and 0°C), tensile strength in splitting at a temperature of 0°C, shear resistance indicators (coefficient of internal friction of adhesion in shear), as shown in the Equation 5:

$$k_{oper} = \sqrt[3]{k_{watr} \cdot k_c \cdot k_{dur}} \qquad (5)$$

where $K_{oper}$ is the coefficient of operational properties characterizing water resistance, fatigue life, resistance to the formation of a track.

The results of the calculation are presented in Table 9.

**T a b l e 9. Generalized criteria for CNT-modified polymer-asphalt concrete**

| Weight factor value | Reference | Sample 2 | Sample 3 |
|---|---|---|---|
| b1=0.3 and b2=0.7 | 1.00 | 1.90 | 1.94 |
| b1=0.4 and b2=0.6 | 1.00 | 1.87 | 1.88 |
| b1=0.5 and b2=0.5 | 1.00 | 1.85 | 1.83 |
| b1=0.6 and b2=0.4 | 1.00 | 1.82 | 1.78 |
| b1=0.7 and b2=0.3 | 1.00 | 1.80 | 1.73 |

Table 9 shows that the developed CNTs-modified polymer asphalt concrete (Sample 2, 3) is more effective in comparison with the traditional composition of polymer asphalt concrete. It has been established that the use of single-walled carbon nanotubes (Sample 2, 3) allows to increase efficiency to 90%.

## CONCLUSIONS

CNTs-modified polymer-bitumen binder has been successfully developed. PBB modified with CNT is characterized by high adhesion and cohesion indicators. To obtain the same effect, CNTs should be used in a much smaller amount (0.1–0.5 wt%) than fly ash or basalt dust. CNTs increase the dynamic viscosity (10%), strengthen, and increase the stability of the binder structure under load. Modification of the bituminous binder with CNTs resulted in an increase in the softening temperature (24%), a decrease in the brittleness temperature (20%) and a 24% and 30% increase in elasticity at 25°C and 0°C, respectively. CNTs stabilize the structure of asphaltene-resin complexes by creating CNT structural elements (physical barriers) that prevent ARC coagulation. Moreover, CNTs increase the dispersion of ARC particles in the range up to 0.8 μm by 30%, which increases the viscosity and consequently reduces delamination and increases the stability of PBB. In addition, CNTs shorten the time to form the PBB structure by 33%, while the cohesive strength increases by 40%. CNTs also function as a stabilizer and aging inhibitor of PBB, contributing to a 10-fold slowdown in its degradation processes compared to classic formulations. It has been proven that a strong, heat-resistant, and waterproof layer is formed on the surface of mineral grains, which allows obtaining asphalt concrete with improved strength and deformability properties.

In polymer-modified asphalt concrete with the addition of CNTs, thermal oxidation processes occur with lower intensity, which results in significantly slower degradation during aging compared to conventional polymer-modified asphalt concrete. The use of polymer-modified base binder (PMB) showed a 20% decrease in the strength of asphalt concrete at a temperature of 20°C after 3 hours of heating, while the use of PMB with CNTs showed a decrease of only 4%. In addition, the initial compressive strength at a temperature of 50°C changed by 23.3% and 3%, respectively. As a result of the conducted studies, the composition of asphalt concrete with improved physical, mechanical and operational properties was developed, which can be used on roads of all technical categories in any road and climatic zone of Ukraine.

*ACKNOWLEDGEMENT*

*The authors gratefully recognize the financial support from the Science and Technology Department of Ningxia, the Scientific Research Fund of North Minzu University (No. 2020KYQD40).*

***Authors contribution***

Authors' contributions are equal.

***Funding***

This research was funded by the Ministry of Education and Science: implementation doctorate program SD/1/2020 and 2020KYQD40 fund from Science and Technology Department of Ningxia, the Scientific Research Fund of North Minzu University.

***Conflict of interest***

The authors declare no conflict of interest.

## REFERENCES

[1] Bunsell A.R., Renard J.: "Fundamentals of fiber reinforced composite materials", CRC Press, Boca Raton, 2005.

[2] Krayushkina K., Khymeryk T., Bieliatynskyi A.: *IOP Conference Series: Materials Science and Engineering* **2019**, *708*, 012088. https://doi.org/10.1088/1757-899X/708/1/012088

[3] Yang S., Bieliatynskyi A., Trachevskyi V. *et al.: International Journal of Concrete Structures and Materials* **2023**, *17(1)*, 50. https://doi.org/10.1186/s40069-023-00601-8

[4] Fernandez G.R.: *Cemento e Hormigon* **1976**, *47(506)*, 415.

[5] Sarde B., Patil Y.D.: *Materials Today: Proceedings* **2019**, *18(7)*, 3780. https://doi.org/10.1016/j.matpr.2019.07.316

[6] Hsissou R., Benhiba F., Echihi S. *et al.: Chemical Data Collections* **2021**, *31*, 100619. https://doi.org/10.1016/j.cdc.2020.100619

[7] Beaudoin J.J.: "Handbook of fiber-reinforced concrete: Principles, properties, developments and applications", William Andrew, New York, 1990.

[8] Bhudolia S.K., Perrotey P. G., Joshi, S.C. *et al.: Polymers* **2021**, *13(23)*, 4093. https://doi.org/10.3390/polym13234093

[9] Dharmalingam A.S., Hemmer J., Lectez A.S. *et al.: Composites Part B: Engineering* **2018**, *148*, 235. https://doi.org/10.1016/j.compositesb.2018.05.001

[10] Mei M., Sun L., He Y. *et al.: Composites Communications* **2021**, *23*, 100545. https://doi.org/10.1016/j.coco.2020.100545

[11] Yang S., Bieliatynskyi A., Pershakov V. *et al.: Journal of Polymer Engineering* **2022**, *42(5)*, 458. https://doi.org/10.1515/polyeng-2021-0345

[12] Coutandin S., Wurba A., Luft A. *et al.: Materials Science and Engineering Technology* **2019**, *50(12)*, 1573. https://doi.org/10.1002/mawe.201900074

[13] Bieliatynskyi A., Yang S., Pershakov V. *et al.: European Journal of Environmental and Civil Engineering* **2023**, *27(5)*, 2070. https://doi.org/10.1080/19648189.2022.2110160

[14] Wei K., Liang D., Mei M. *et al.: International Journal of Applied Mechanics* **2018**, *10(10)*, 1850111. https://doi.org/10.1142/S1758825118501119

[15] Bhudolia S.K., Gohel G., Leong K.F. *et al.: Composites Part B: Engineering* **2020**, *203*, 108480. https://doi.org/10.1016/j.compositesb.2020.108480

[16] Hsissou R., Seghiri R., Benzekri Z. *et al.: Composite Structures* **2021**, *262*, 113640. https://doi.org/10.1016/j.compstruct.2021.113640

[17] Polacco G., Stastna J., Biondi D. *et al.: Current Opinion in Colloid and Interface Science* **2006**, *11(4)*, 230.

[18] Zolotarev V.A.: "Properties of bitumen modified with SBS polymers", Kharkiv National Automobile and Highway University, Kharkiv, 2006.

[19] Asphalt Institute and Eurobitume: "The bitumen industry – a global perspective", Asphalt Institute, Lexington, Eurobitume, Brussels, 2011.

[20] Becker Y., Mendez M.P., Rodriguez Y.: *Vision Technological* **2001**, *9(1)*, 39.

[21] Wei K., Liang D., Mei M. *et al.: Composites Part B: Engineering* **2019**, *158*, 1. https://doi.org/10.1016/j.compositesb.2018.09.038

[22] Zolotarev V.A., Bratchun V.I.: "Modified bitumen binders, special bitumen and bitumen with additives in road construction", Kharkiv National Automobile and Highway University, Kharkiv, 2003.

[23] Wei K., Liang D., Mei M. *et al.: Composites Part B: Engineering* **2019**, *166*, 221. https://doi.org/10.1016/j.compositesb.2018.11.143

[24] Mendikute J., Plazaola J., Baskaran M. *et al.: Composites Part B: Engineering* **2021**, *221*, 108973. https://doi.org/10.1016/j.compositesb.2021.108973

[25] Krayushkina K., Prentkovskis O., Bieliatynskyi A. *et al.: Transport* **2012**, *27(2)*, 129. https://doi.org/10.3846/16484142.2012.690093

[26] Takemura K.: "Some properties of concrete using crushed stone pust as fine aggregate" in "The Cement Association of Japan 13th General Meeting Technical Session", (editor Takemura K.), YI Review, Tokyo 2004, p. 81.

[27] Zhang S., Pelligra C.I., Feng X. *et al.: Advanced Materials* **2018**, *30(18)*, 1705794, https://doi.org/10.1002/adma.201705794

[28] Bieliatynskyi A., Yang S., Pershakov V. *et al.: Science and Engineering of Composite Materials* **2022**, *29(1)*, 227. https://doi.org/10.1515/secm-2022-0018

[29] https://online.budstandart.com/catalog/doc-page.html?id_doc=4674 (access date 17.03.2024)

[30] https://online.budstandart.com/catalog/doc-page.html?id_doc=84291 (access date 17.03.2024)

[31] Grace N.F., Singh S.B.: *ACI Structural Journal* **2005**, *102(1)*, 40.

[32] Krayushkina K., Prentkovskis O., Bieliatynskyi A. *et al.: The Baltic Journal of Road and Bridge Engineering* **2016**, *11(1)*, 77. https://doi.org/10.3846/bjrbe.2016.09

*Received 4 VII 2024.*
*Accepted 27 VIII 2024.*

**Stowarzyszenie Wychowanków Politechniki Śląskiej w Gliwicach**
oraz
**Politechnika Śląska Wydział Mechaniczny Technologiczny,**
**Katedra Mechaniki Teoretycznej i Stosowanej,**
**Polskie Towarzystwo Mechaniki Teoretycznej i Stosowanej,**
**Towarzystwo Przetworów Tworzyw Polimerowych**

*zapraszają do udziału w*

**XXI Konferencji Naukowo-Technicznej**
**„POLIMERY I KOMPOZYTY KONSTRUKCYJNE 2024"**
22–25 października 2024 r., Wisła

**Patronat Honorowy Konferencji:**
J. M. Rektor Politechniki Śląskiej – prof. dr hab. inż. Arkadiusz MĘŻYK
**Honorowy Przewodniczący Konferencji:** dr hab. inż. Maciej ROJEK
**Przewodniczący Komitetu Naukowego**: prof. dr hab. inż. Gabriel WRÓBEL
**Przewodnicząca Komitetu Organizacyjnego**: dr hab. inż. Małgorzata SZYMICZEK, prof. PŚ
**Tematyka konferencji:**

- Kompozyty konstrukcyjne i ich własności
- Nanokompozyty i materiały gradientowe o osnowie polimerowej
- Materiały polimerowe o specjalnych własnościach
- Mechanika materiałów polimerowych
- Metody badań materiałów polimerowych (w tym nieniszczące)
- Biomateriały polimerowe
- Powłoki polimerowe
- Przetwórstwa materiałów polimerowych

Wybrane prace rekomendowanych przez Komitet Naukowy (za dodatkową opłatą) zostaną opublikowane w czasopismach: *Journal of Achievements in Materials and Manufacturing Engineering, Archives of Materials Science and Engineering, Polimery, Archives of Acoustics, Advances in Science and Technology Research Journal, Archives of Foundry Engineering*

**Ważne terminy:**
Zgłoszenie udziału – 15 września 2024 r.
Nadesłanie streszczeń – 30 września 2024 r.
Dokonanie opłaty – 30 września 2024 r.
**Opłata konferencyjna:**
Opłata za uczestnictwo: 2500,00 PLN (575 EUR) - pokój dwuosobowy
Opłata za uczestnictwo: 2700,00 PLN (620 EUR) - pokój jednoosobowy
Koszt opłaty osoby towarzyszącej: 2100,00 PLN (490 EUR)*⁾
Opłata uczestnictwa doktorantów i studentów: 2200,00 PLN (510 EUR) – pokój dwuosobowy
Opłata obejmuje: zakwaterowanie, wyżywienie, materiały konferencyjne i imprezy towarzyszące
*⁾ bez materiałów konferencyjnych
**Miejsce konferencji**: **Hotel Vestina***,** ul. Malinka 35, 43-460 Wisła, Polska
**Informacje:** composites@icepc.com.pl, tel. +48 32 237 12 43 lub +48 32 237 13 62
**www.icepc.com.pl**